Nano Res (2010) 3: 490–495
DOI 10.1007/s12274-010-0009-5
Research Article

Holed Nanostructures Formed by Aluminum Droplets on a GaAs Substrate

Alvason Zhenhua Li (✉), Zhiming M. Wang (✉), Jiang Wu, and Gregory J. Salamo

Institute of Nanoscale Science and Engineering, University of Arkansas, Fayetteville, Arkansas 72701, USA

Received: 5 April 2010 / Revised: 5 May 2010 / Accepted: 12 May 2010

ABSTRACT

We have studied the morphology evolution of holed nanostructures formed by aluminum droplet epitaxy on a GaAs surface. Unique outer rings with concentric inner holed rings were observed. Further, an empirical equation to describe the size distribution of the outer rings in the holed nanostructures has been established. The contour line generated by the equation provides physical insights into quantum ring formation by droplets of group Ⅲ materials on Ⅲ–Ⅴ substrates.

KEYWORDS

Droplet epitaxy, aluminum droplets, MBE, GaAs, holed nanostructures

1. Introduction

Self-organized semiconductor quantum nanostructures have attracted extensive interest and intensive research owing to their great potential applications in basic physics and advanced solid state devices—for example, quantum rings for Aharonov–Bohm interferometers and entangled quantum dots for quantum information processes [1–7]. Among the different self-organized epitaxial growth methods, droplet epitaxy has considerable potential for the fabrication of such peculiar nanostructures and advanced semiconductor devices [8, 9]. A significant advantage of droplet epitaxy growth is its flexibility in that it is applicable to both lattice-mismatched and lattice-matched systems. Since the initial work by Koguchi et al. [10], various dot-like [11–13], ring-like [14–17], and hole-like nanostructures [18–20] have been observed on Ⅲ–Ⅴ semiconductors. Here, "hole-like" or "holed" nanostructures specifically refer to a ring nanostructure with a hole beneath the substrate, while "ring-like" nanostructure specifically refers to a ring nanostructure with a hole above the substrate. The holed nanostructures, first demonstrated by Wang et al. [21], are particularly promising candidates for the formation of uniform and low-density quantum rings [22–24]. However, all the previously published work has involved the formation of nanostructures from gallium (Ga) or indium (In) droplets [10–24], and there has been no report of aluminum (Al) droplets on GaAs substrates, although there have been a few of papers involving Al droplets [11, 25]. Investigation of the nanostructures formed from Al droplets will not only enrich our knowledge of group Ⅲ droplet epitaxy and facilitate an understanding of the mechanism of droplet epitaxial growth but should also create unique nanostructures due to the fact that Al is the most chemically reactive element among the group Ⅲ metals. Further investigation is needed to

Address correspondence to Alvason Zhenhua Li, alvali@uark.edu; Zhiming M. Wang, zmwang@uark.edu

provide a solid understanding of such a simple and novel molecular beam epitaxy (MBE) growth process [26]. In this paper, the formation of double ring holed nanostructures by aluminum (Al) droplet epitaxy on GaAs substrates is presented in detail for the first time. The relationship between the formation of nanorings under various annealing conditions and arsenic background pressures are investigated. This work focuses on a topography/morphology study instead of a quantum confinement study.

2. Experimental procedures

Samples were grown on semi-insulating GaAs(001) substrates by MBE. Following thermal deoxidization, a 500 nm thick GaAs buffer layer was grown at 580 ˚C. The substrate was cooled to 500 ˚C. Under an ultra-low arsenic background pressure of 5.0×10^{-9} Torr, an Al molecular beam was supplied to the substrate surface, leading to Al droplet formation. The total amount of deposited Al was equivalent to 3 monolayers (ML) of AlAs grown at a growth rate of 1 ML/s. Keeping the arsenic background pressure in the MBE growth chamber ultra-low (around 5.0×10^{-9} Torr), the Al droplets were annealed at higher annealing temperatures or under different arsenic flux conditions as described later.

3. Results

Figure 1 illustrates three atomic force microscope (AFM) images (in tapping mode) of samples after annealing under various conditions: (a) 0 s at 500 ˚C without an As flux; (b) 60 s at 500 ˚C with an As flux; (c) when the temperature was ramped up from 500 to 620 ˚C quickly (50 ˚C/min), then kept for 60 s at 620 ˚C without an As flux. These annealing experiments demonstrate the evolution of the holed nanostructures.

As shown in Fig. 1(a), there are 11 large holed nanostructures of similar size (100 nm ± 10 nm) together with nearly a hundred small holed nanostructures of various size (40 nm ± 20 nm). The sizes of the Al holed nanostructures vary more widely than those of Ga holed nanostructures observed in previous work

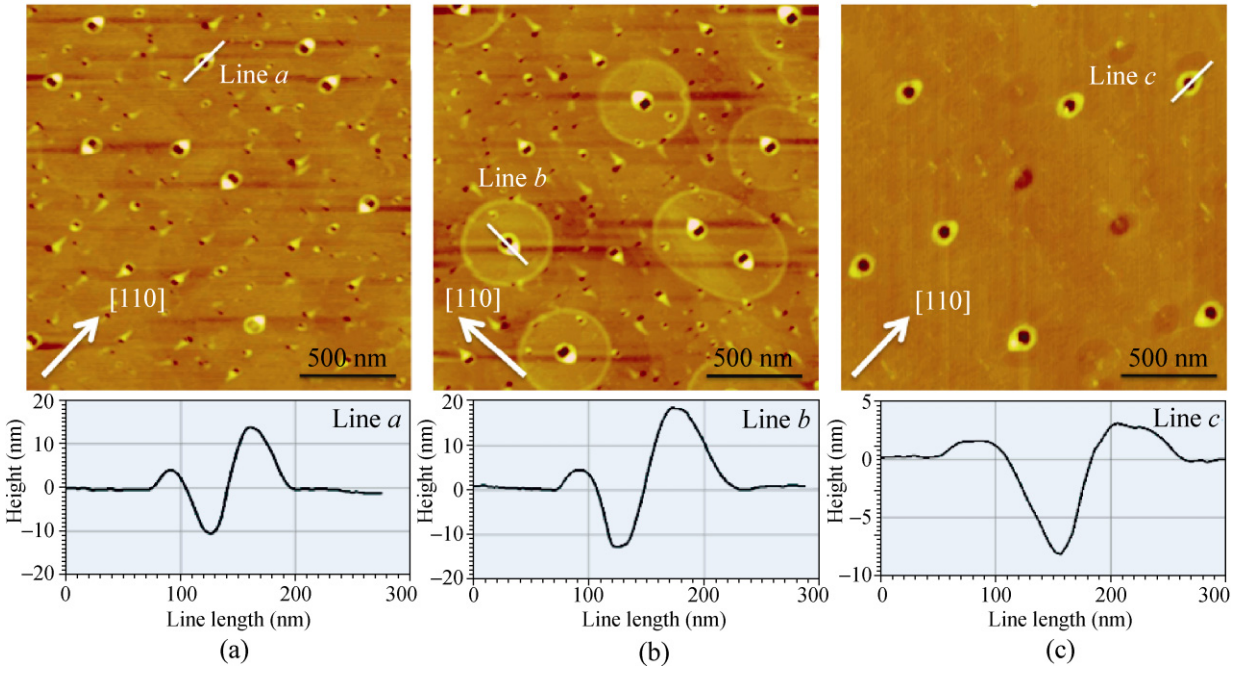

Figure 1 AFM images (each is 2 μm × 2 μm) of 3 monolayers (ML) of Al after annealing under various conditions, with the typical AFM line-scanning profile along [110] shown under each AFM image: (a) after 0 s at 500 ˚C without an As flux, single holed rings have formed at the sites of large droplets and small holed dots have formed at the sites of small droplets; (b) after 60 s at 500 ˚C under an As flux of 1.0×10^{-6} Torr as background pressure, outer rings which are concentric with the inner holed rings have formed; (c) after 60 s at 620 ˚C without an As flux, the inner holed rings have become larger and smooth, and the small holed dots have disappeared

[18–21]. This suggests that the deposited Al atoms are more chemically reactive and less mobile than Ga atoms deposited on a GaAs substrate.

In the presence of an arsenic supply, the radial diffusion zones from the large droplets are clearly observed as shown in Fig. 1(b). Significantly, an outer ring which is concentric with its inner holed ring is formed, as indicated in the AFM scanning profile (line *b* in Fig. 1(b)). Further details of the influence of arsenic on the building up of the edge of the outer ring of the holed nanostructures will follow.

After increasing the annealing temperature, the small holed nanostructures disappeared, as shown in Fig. 1(c). Meanwhile, comparison of Figs. 1(a) and 1(b) shows that the holed rings are expanded and smoothed at the higher annealing temperature (Fig. 1(c)), and the depth of the holes becomes shallower as indicated by a comparison of AFM scanning profiles (line *a* and line *c*).

The unique double ring holed nanostructure were examined in more detail by scanning electron microscopy (SEM) and AFM. Smooth and symmetrical double ring nanostructures are clearly observed, as shown in Figs. 2(a) and 2(b). Based on the AFM scanning line profile from a typical Al double ring in Fig. 2(c), a simple schematic diagram can be derived to characterize the double ring in cross-sectional view, as shown in Fig. 2(d). In this diagram, we assume the initial Al droplet has the same behavior as a gallium or indium droplet in that the initial sizes and shapes of the holed nanostructures directly correspond to the initial sizes of the droplets [11, 21, 22, 25] with the following results: (1) the inner ring diameter is the same magnitude as the diameter of the initial droplet; (2) the central hole depth is the same magnitude as the height of the initial droplet; (3) the inner ring height is ~6 nm while the outer ring height is reduced to half this value; (4) the distance between the inner and outer rings is 200 nm ± 20 nm. It should be noted that the large flat spacing between Al concentric double rings

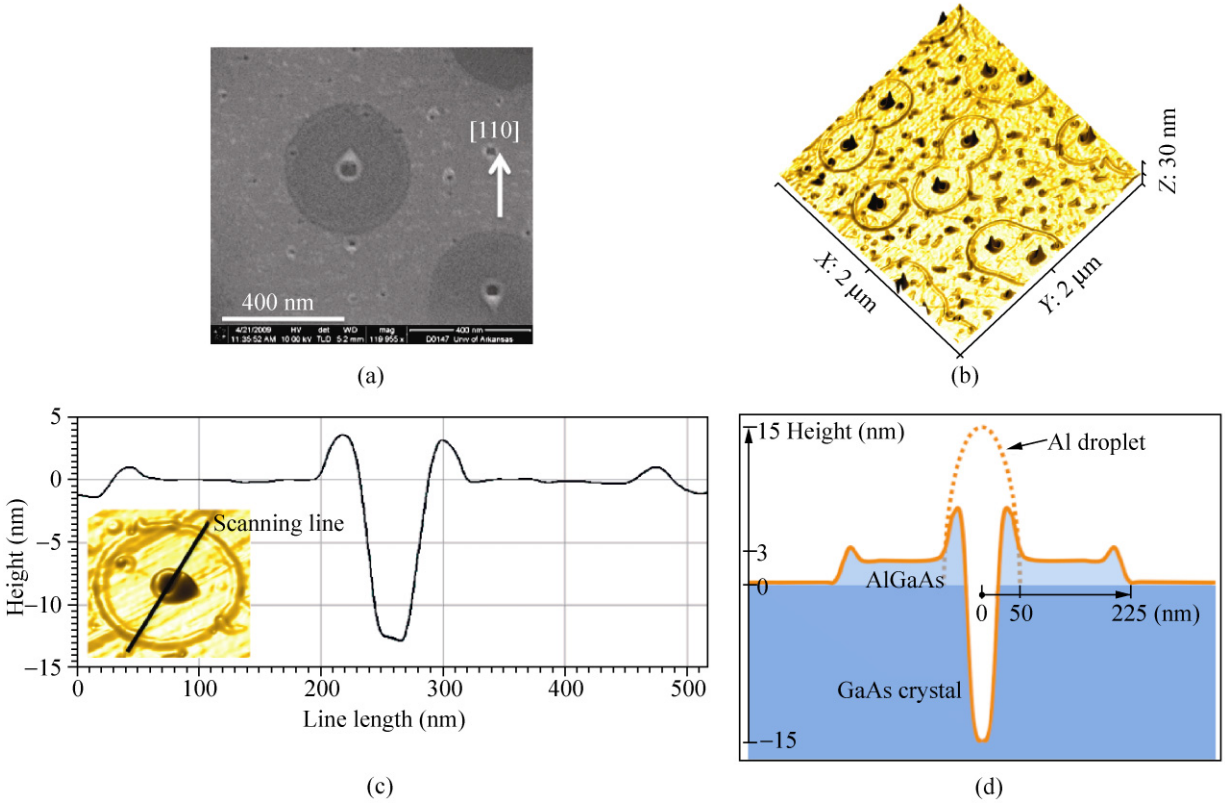

Figure 2 The analysis of a typical double ring holed nanostructure. (a) a SEM image in top-view. (b) An AFM image in 3-D view. (c) An AFM scanning-line profile from a typical double ring; the AFM image in the insert shows that the corresponding scanning line is along the [1$\bar{1}$0] direction. (d) A schematic diagram of a typical double ring holed nanostructure in cross-sectional view along the [1$\bar{1}$0] direction: the orange dashed line indicates the initial Al droplet, the orange line indicates the formation of an AlGaAs double ring with a center hole depth which is the same magnitude as the height of the initial droplet. The dark blue region indicates the GaAs substrate

observed in this work is one distinguishing feature from the ordinary compact concentric double rings or multiple concentric nanorings observed for Ga droplet epitaxy [17].

A quantitative analysis of the double ring structures, based on 5 μm × 5 μm large area AFM images was carried out (Fig. 3(a)) and showed that the double ring density is about 2×10^8/cm^2. As shown in Fig. 3(b), the histograms of the sizes of both the inner holed ring and outer diffusion ring have a normal distribution with a relatively narrow ring size distribution. The diameter of the inner ring is 100 nm ± 10 nm while the diameter of the outer ring is 450 nm ± 40 nm.

4. Discussion

The AFM results in Figs. 1(a) and 1(b) indicate that the nature of the inner holed nanostructures does not depend significantly on the As flux, which suggests that the main structure of the inner hole is the direct result of the reaction between the initial Al droplet and the underlying GaAs substrate due to the high chemical reactivity of Al. Furthermore, the inner rings are asymmetric along the ± [110] direction while the outer rings exhibit radial symmetry, which emphasizes that the diffusion mechanism for the inner rings differs from that for the outer rings. Further analysis

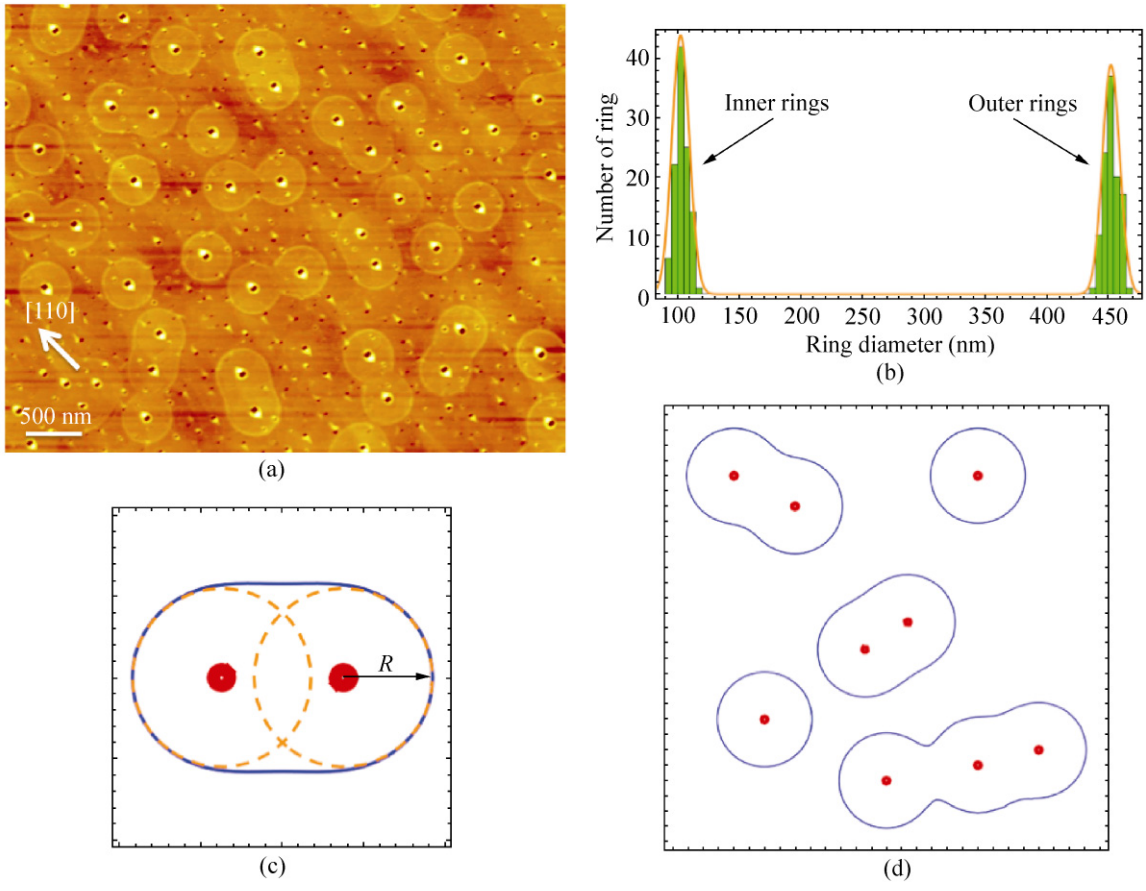

Figure 3 Analysis and simulation of outer ring size distribution and profile. (a) A typical AFM image of the double ring holed nanostructures. (b) The histogram shows the size distribution of the inner holed rings and the outer diffusion rings. The sizes of both the inner and outer rings follow a Gaussian distribution as indicated by the yellow curves. (c) The red dot indicates the diffusion source, and the orange dashed circle generated by Eq. (1) indicates the expanding diffusion ring with a characteristic diffusion radius "*R*" in case of a single diffusion source. The blue elliptical shape generated by Eq. (2) indicates the net diffusion ring when two diffusion sources interact with each other. (d) The simulation of the profile of the outer rings: the red dots indicate the diffusion sources, and the blue lines are the contour lines generated by the randomly distributed diffusion sources based on Eq. (2)

of the composition of these inner and outer rings will provide important details of these mechanisms.

The outer ring profile from one diffusion source can be modeled as the contour line that is generated by a two-dimensional Gaussian function having a constant value R

$$f(x,y) = A\mathrm{e}^{-((x-x_0)^2+(y-y_0)^2)} = R \quad (1)$$

where the constant R is the radius of the expanding diffusion circle from a single inner isotropic diffusion source, (x_0, y_0) is the center of the diffusion source, and the coefficient A is related to the specific growth conditions. Then, for a system with more than one diffusion source, the resulting outer ring profiles can be simply simulated as the contour line generated by the following equation:

$$f(x,y) = A\sum_{i=1}^{N}\mathrm{e}^{-((x-x_i)^2+(y-y_i)^2)} = R \quad (2)$$

where both R and A retain the same value as for the case of a single diffusion source, N is the total number of diffusion sources, and (x_i, y_i) is the center of diffusion source i. We assume that all the diffusion sources are the same and giving concurrent diffusive processes.

For example, as shown in Fig. 3(c), when two diffusion sources are close to each other, the resulting outer ring profile can be described as an elliptical shape, which is the same as that observed experimentally. Furthermore, as shown in Fig. 3(d), the simulation result for random diffusion sources is reasonably consistent with the experimental observations.

It is also noteworthy that, based on Eq. (2), by omitting crystalline anisotropic effects and restricting our attention to radial diffusion and assuming all the diffusion sources are the same, we are able to reproduce the edge profile features of the outer rings formed with concurrent diffusion sources. This simple simulation provides a certain amount of information: (1) the pattern of Al droplet diffusion with chemical reaction on the GaAs substrate has a characteristic diffusion radius; (2) the mutual interaction between concurrent diffusion sources can be described by a Gaussian function which is the Green's function for the isotropic diffusion equation.

5. Conclusions

We have investigated the evolution of holed nanostructures on a GaAs surface by aluminum droplet epitaxy. The holed nanostructures were tuned by raising the annealing temperature and varying the arsenic flux. Peculiar outer rings concentric with the inner holed rings were formed by using an appropriate arsenic flux, and a mathematically simple empirical equation was established in order to examine the edge profile of the outer ring. It is expected that this equation will provide further insight into the growth mechanism of droplet epitaxy.

Acknowledgements

The authors gratefully acknowledge the financial support by the MRSEC Program of NSF Grant (DMR-0520550). The valuable comments of Tim Morgan are gratefully acknowledged.

References

[1] García, J. M.; Medeiros-Ribeiro, G.; Schmidt, K.; Ngo, T.; Feng, J. L.; Lorke, A.; Kotthaus, J.; Petroff, P. M. Intermixing and shape changes during the formation of InAs self-assembled quantum dots. *Appl. Phys. Lett.* **1997**, *71*, 2014–2016.

[2] Mlakar, T.; Biasiol, G.; Heun, S.; Sorba, L.; Vijaykumar, T.; Kulkarni, G. U.; Spreafico, V.; Prato, S. Conductive atomic force microscopy of InAs/GaAs quantum rings. *Appl. Phys. Lett.* **2008**, *92*, 192105-1-3.

[3] Szafran, B. Correlated persistent currents in a stack of semiconductor quantum rings. *Phys. Rev. B* **2008**, *77*, 235314.

[4] Dai, J. -H, Lee, J. -H.; Lin, Y. -L.; Lee, S. -C. In(Ga)As quantum rings for terahertz detectors. *Jpn. J. Appl. Phys.* **2008**, *47*, 2924–2926.

[5] Bruno-Alfonso, A.; Latgé, A. Quantum rings of arbitrary shape and non-uniform width in a threading magnetic field. *Phys. Rev. B* **2008**, *77*, 205303-1-8.

[6] Chi, F.; Li, S. -S. Spin-polarized transport through an Aharonov-Bohm interferometer with Rashba spin-orbit

interaction. *J. Appl. Phys.* **2006**, *100*, 113703.

[7] Fomin, V. M.; Gladilin, V. N.; Klimin, S. N.; Devreese, J. T.; Kleemans, N. A.; Koenraad, P. M. Theory of electron energy spectrum and Aharonov–Bohm effect in self-assembled $In_xGa_{1-x}As$ quantum rings in GaAs. *Phys. Rev. B.* **2007**, *76*, 235320.

[8] Pomraenke, R.; Lienau, C.; Mazur, Y. I.; Wang, Z. M.; Liang, B.; Tarasov, G. G.; Salamo, G. Near-field optical spectroscopy of GaAs/$Al_yGa_{1-y}As$ quantum dot pairs grown by high-temperature droplet epitaxy. *J. Phys. Rev. B.* **2008**, *77*, 075314.

[9] Belhadj, T.; Kuroda, T.; Simon, C. -M.; Amand, T.; Mano, T.; Sakoda, K.; Koguchi, N.; Marie, X.; Urbaszek, B. Optically monitored nuclear spin dynamics in individual GaAs quantum dots grown by droplet epitaxy. *Phys. Rev. B*. **2008**, *78*, 205325.

[10] Koguchi, N.; Ishige, K. Growth of GaAs epitaxial microcrystals on an s-terminated GaAs substrate by successive irradiation of Ga and As molecular-beams. *Jpn. J. Appl. Phys*. **1993**, *32*, 2052–2058.

[11] Sablon, K. A.; Wang, Z. M.; Salamo, G. J. Composite droplets: Evolution of InGa and AlGa alloys on GaAs(100). *Nanotechnology* **2008**, *19*, 125609.

[12] Kim, J. S.; Jeong, M. S.; Byeon, C. C.; Ko, D. K.; Lee, J.; Kim, J. S.; Koguchi, N. GaAs quantum dots with a high density on a GaAs (111)A substrate. *Appl. Phys. Lett.* **2006**, *88*, 241911.

[13] Heyn, C.; Stemmann, A.; Schramm, A.; Welsch, H.; Hansen, W.; Nemcsics, Á. Regimes of GaAs quantum dot self-assembly by droplet epitaxy. *Phys. Rev. B*. **2007**, *76*, 075317.

[14] Pankaow, N.; Panyakeow, S.; Ratanathammaphan, S. Formation of $In_{0.5}Ga_{0.5}As$ ring-and-hole structure by droplet molecular beam epitaxy. *J. Crystal Growth* **2009**, *311*, 1832–1835.

[15] Zhao, C.; Chen, Y. H.; Xu, B.; Tang, C. G.; Wang, Z. G.; Ding, F. Study of the wetting layer of InAs/GaAs nanorings grown by droplet epitaxy. *Appl. Phys. Lett.* **2008**, *92*, 063122.

[16] Tong, C. Z.; Yoon, S. F. Investigation of the fabrication mechanism of self-assembled GaAs quantum rings grown by droplet epitaxy. *Nanotechnology* **2008**, *19*, 365604.

[17] Somaschini, C.; Bietti, S.; Koguchi, N.; Sanguinetti, S. Fabrication of multiple concentric nanoring structures. *Nano Lett.* **2009**, *9*, 3419–3424.

[18] Stemmann, A.; Heyn, C.; Köppen, T.; Kipp, T.; Hansen, W. Local droplet etching of nanoholes and rings on GaAs and AlGaAs surfaces. *Appl. Phys. Lett.* **2008**, *93*, 123108.

[19] Heyn, C.; Stemmann, A.; Hansen, W. Dynamics of self-assembled droplet etching. *Appl. Phys. Lett.* **2009**, *95*, 173110.

[20] Li, A. Z.; Wang, Z. M.; Wu, J.; Xie, Y.; Sablon, K. A.; Salamo, G. J. Evolution of holed nanostructures on GaAs (001). *Cryst. Growth Des.* **2009**, *9*, 2941–2943.

[21] Wang, Z. M.; Liang, B. L.; Sablon, K. A.; Salamo, G. J. Nanoholes fabricated by self-assembled gallium nanodrill on GaAs(100). *Appl. Phys. Lett.* **2007**, *90*, 113120.

[22] Liang, B. L.; Wang, Z. M.; Lee, J. H.; Sablon, K.; Mazur, Y. I.; Salamo, G. J. Low density InAs quantum dots grown on GaAs nanoholes. *Appl. Phys. Lett.* **2006**, *89*, 043113.

[23] Alonso-Gonzalez, P.; Alen, B.; Fuster, D.; Gonzalez, Y.; Gonzalez, L.; Martinez-Pastor. Formation and optical characterization of single InAs quantum dots grown on GaAs nanoholes. *J. Appl. Phys. Lett.* **2007**, *91*, 163104.

[24] Alonso-González, P.; Fuster, D.; González, L.; Martín-Sánchez, J.; González, Y. Low density InAs quantum dots with control in energy emission and top surface location. *Appl. Phys. Lett.* **2008**, *93*, 183106.

[25] Heyn, C.; Stemmann, A.; Köppen, T.; Strelow, C.; Kipp, T.; Grave, M.; Mendach, S.; Hansen, W. Highly uniform and strain-free GaAs quantum dots fabricated by filling of self-assembled nanoholes. *Appl. Phys. Lett.* **2009**, *94*, 183113.

[26] Li, X. L.; Yang, G. W. Growth mechanisms of quantum ring self-assembly upon droplet epitaxy. *J. Phys. Chem. C* **2008**, *112*, 7693–7697.